



Exergy and reliability analysis of wind turbine systems: A case study

Onder Ozgener^a, Leyla Ozgener^{b,*}

^a*Solar Energy Institute, Ege University, TR-35100, Bornova, Izmir, Turkey*

^b*Department of Mechanical Engineering, Faculty of Engineering, Celal Bayar University, TR-45140, Muradiye, Manisa, Turkey*

Received 10 March 2006; accepted 28 March 2006

Abstract

The present study undertakes an exergy and reliability analysis of wind turbine systems and applies to a local one in Turkey: the exergy performance and reliability of the small wind turbine generator have been evaluated in a demonstration (1.5 kW) in Solar Energy Institute of Ege University (latitude 38.24 N, longitude 27.50 E), Izmir, Turkey. In order to extract the maximum possible power, it is important that the blades of small wind turbines start rotating at the lowest possible wind speed. The starting performance of a three-bladed, 3 m diameter horizontal axis wind turbine was measured in field tests. The average technical availability, real availability, capacity factor and exergy efficiency value have been analyzed from September 2002 to November 2003 and they are found to be 94.20%, 51.67%, 11.58%, and 0–48.72%, respectively. The reliability analysis has also been done for the small wind turbine generator. The failure rate is high to an extent of $2.28 \times 10^{-4} \text{ h}^{-1}$ and the factor of reliability is found to be 0.37 at 4380 h. If failure rate can be decreased, not only this system but also other wind turbine systems of real availability, capacity factor and exergy efficiency will be improved.

© 2006 Elsevier Ltd. All rights reserved.

Keywords: Efficiency; Energy; Exergy; Renewable energy; Reliability analysis; Wind energy

*Corresponding author. Tel.: +90 236 24121 44/240; fax: +90 232 388 6027.

E-mail addresses: onder.ozgener@ege.edu.tr (O. Ozgener), leyla.ozgener@bayar.edu.tr (L. Ozgener).

Contents

1. Introduction	1812
2. Case study	1815
2.1. Experimental setup	1815
2.2. Measurements.	1816
2.3. System operation	1818
3. Analysis	1818
3.1. Mean time between failures	1819
3.2. Capacity factor.	1820
3.3. Performing exergy analysis of the system studied	1820
4. Results and discussions	1821
5. Conclusions	1824
References	1825

1. Introduction

The reliability aspects of alternative sources of energy are of growing importance. This is largely because of the fact that renewable energy sources are contributing to major power systems more than in the past [1]. Turkey's total theoretically available potential for wind power is found to be about 88,000 MW/yr. Besides this, Turkey's wave power potential is estimated to be around 18,500 MW/yr, with an average wave energy capacity of 140 billion kWh annually. These figures indicate that Turkey has considerable potential for generating electricity from wind and wave power [2,3]. Today, distributed small wind electric systems can make a significant contribution to Turkey's energy needs. To date, four wind power plants were installed with a total capacity of 20.1 MW in Turkey, while a wind power plant with a total capacity of 39.2 MW will be commissioned in 2006 summer, at Cesme, Izmir. Due to recent increase in the price of fossil fuels, it is becoming ever more costly to provide energy for our abodes, and there is also the fact pollution is being created to provide this energy. This study aims to develop more efficient and more useful small wind turbine system (SWTS) for rural areas increasing energy and exergy efficiencies, and decreasing costs of stand-alone and wind systems in the Aegean Region, Turkey.

Renewable energy is abundant and its technologies are well established to provide complete security of energy supply [4]. Among renewable energy sources, wind energy plays an important role. From the late 1800s to the early 1900s, thousands of US farmers and ranchers used windmills to pump water, grind grain, charge batteries, and provide power for radios, lights, and washing machines. The use of windmills to provide electric power died out in the early 1930s when the Rural Electrification Administration made cheap electricity generated at centralized power stations available to farms and ranches across the country. The cost of electricity in many areas is spiraling upwards and weak electrical grids make power to remote farms and ranches less reliable than in the past. Even urban homeowners are faced with unexpected jumps in power costs [5].

Researchers estimate that 50% of the US has enough wind resources for small turbine development and 60% of US homes are located in those wind resource areas. Using small wind turbines, farmers, ranchers, and homeowners can reduce their utility bills, stabilize their electricity supplies, and contribute to nation energy supply to play an important role in securing our energy future. Distributed wind electric systems represent an opportunity

Nomenclature

A	rotor swept area (m^2)
C_M	momentum factor of rotor (dimensionless)
C_P	power coefficient (energy conversion ratio) (dimensionless)
$C_{P,a}$	air specific heat (kJ/kg K)
$C_{P,v}$	water vapor specific heat (kJ/kg K)
Ex_{dest}	exergy destruction (W, kW)
H	height (m)
H_{ref}	reference height (m)
I	phase currents (A)
\dot{m}	mass flow rate of air (kg/s)
\dot{m}_w	mass flow rate of water vapor in air (kg/s)
P	pressure (kPa)
ΔP	pressure difference at state 1 and 2 (Pa)
R	maximum rotor radius (m)
R_a	gas constant (kJ/kg K)
R_v	vapor constant (kJ/kg K)
Δt_i	yearly cumulative time (h/year)
T	temperature (K, $^{\circ}\text{C}$)
T_0	reference temperature (K, $^{\circ}\text{C}$)
V_r	local wind velocity (m/s)
V_{ref}	wind velocity at reference height (m/s)
V_{LL}	phase to phase voltage (V)
V_{LN}	phase voltages (V)
W	available power (W)
W_a	actual power (active power at generator output) (W, kW)
W_e	power at inverter output (W, kW)
W_u	useful power from turbine (W, kW)
W_{aw}	actual work of the SWTS (kWh)
W_{teo}	theoretical work potential of the SWTS (kWh)
1,2	state points

Greek letters

ω	angular speed of rotor (rad/s); humidity ratio ($\text{kg}_{\text{water}}/\text{kg}_{\text{air}}$)
ω_0	humidity ratio at reference point ($\text{kg}_{\text{water}}/\text{kg}_{\text{air}}$)
η	energy efficiency (dimensionless)
ε	exergy efficiency (dimensionless)
ψ_a	specific exergy of air (kJ/kg)
λ	tip speed ratio (dimensionless); constant failure rate (h)
ρ	air density (kg/m^3)
μ	hellman coefficient (dimensionless)
Σ	Total

Abbreviations

HAWT horizontal axis wind turbine
 LCD liquid crystal display
 NACA National Advisory Committee of Aeronautics
 MTBF mean time between failure
 PBL planetary boundary layer
 P.F. ($\cos \Psi$) power factor (dimensionless)
 SWTs small wind turbine (windmill) system

for some nation especially American households to return to the energy independence of a past century [5].

Small wind turbines need to be affordable, reliable and almost maintenance free for the average person to consider installing one. This often means a sacrifice of optimal performance for simplicity in design and operation. Thus, rather than using the generator as a motor to start and accelerate the rotor when the wind is strong enough to begin producing power, small wind turbines rely solely on the torque produced by the wind acting on the blades. Furthermore, small wind turbines are often located where the generated power is required, and not necessarily where the wind resource is best. In these low or unsteady wind conditions, slow starting reduces the total energy generated. Also, a stationary wind turbine fuels the perception of wind energy as an unreliable energy source [6].

Wind energy researches on its applications and effects have rapidly increased in the world (e.g. [7–24]), so efficiency of wind energy constructions is getting importance. Theoretically, maximum benefit is from 59.2% blowing wind according to the Betz Criteria. Today, available wind energy ratio reaches about on average 40–45% in modern wind turbine types. In order to extract the maximum possible power, it is important that the blades of small wind turbines start rotating at the lowest possible wind speed [6].

The aerodynamic and structural design of rotors for horizontal axis wind turbines (HAWTs) is a multi-disciplinary task, involving conflicting requirements on, for example, maximum performance, minimum loads and minimum noise. The wind turbine operates in very different conditions from normal variation in wind speed to extreme wind occurrences. Optimum efficiency is not obtainable in the entire wind speed range, since power regulation is needed to prevent generator burnout at high wind speeds. Optimum efficiency is limited to a single-design wind speed for stall regulated HAWTs with fixed speed of rotation. The development of suitable optimization methods for geometric shape design of HAWT rotors is therefore a complex task that involves off-design performance and multiple considerations on concept, generator size, regulation and loads [8].

NACA 63-nnn series blades can be preferred to other examples in applications for performance improvement, because of the fact that these profiles have shown excellent properties for wind turbine blades and their average power coefficients are higher than other blades [11,12]. Wind turbines very often have to operate in high turbulence related, for example, with lower layers atmospheric turbulence or wakes of other wind turbines. Most available data on airfoil aerodynamics concerns mainly aeronautical applications, which are characterized by a low level of turbulence (generally less than 1%) and low angles of attack [9].

The presented reliability analysis section was especially inspired by publication of [10], in which for the first time the performance and reliability of the wind turbine generators have been evaluated in a demonstration wind farm. The reliability analysis has also been done for the small horizontal axis wind turbine generator, three NACA series bladed in Solar Energy Institute, Izmir, Turkey. In addition, we examine exergy efficiencies and their trends of the wind turbine system according to wind speeds and different temperatures of blowing air and also briefly describe an easy-to-follow procedure for the exergy analysis of wind turbine systems and how to apply this procedure to assess the system performance by calculating exergy destruction. The case study, the small wind turbine system (SWTS) processing, is selected for analysis assessment and evaluation purposes.

2. Case study

2.1. Experimental setup

A test facility was constructed to study the requiring electricity needs environment lights of Solar Energy Institute during night's conditions. Consumed energy for environment lights purposes depends on seasons and daily changing climatic conditions. Figs. 1 and 2 illustrate a schematic diagram of the constructed experimental system and a view of system. The main characteristics of the elements of the experimental setup are given in Table 1. Moreover, Table 2 shows that thermal data used the case study. The experimental system consists of five major parts as follows: (a) Electronics; charge controller, power conversion, inverter, charger, warmth control equipment, thermocouple (thermic), (b) storage batteries, (c) mechanics: tower, nose cone, yaw bearing, slip rings, tail, vane, nacelle assembly, (d) 1.5 kW non-synchrony generator (alternator) and blades, (e) environmental

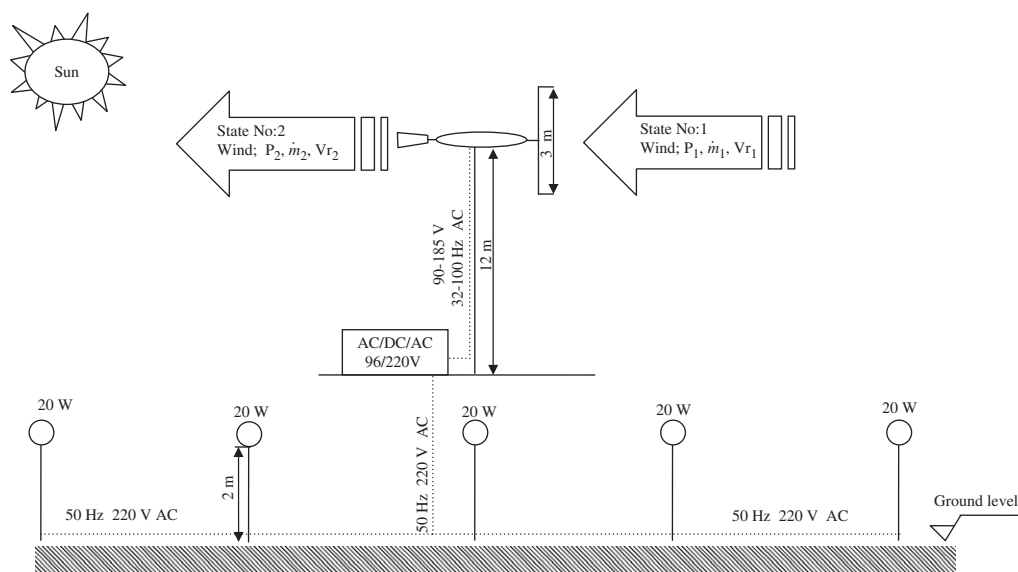


Fig. 1. A schematic of the SWTS.



Fig. 2. A view of SWTS.

energy saving five lamps total power 100 W, (f) five moving and light sensors for energy saving.

The random or stochastic nature of wind is the single most unique design constraint that differentiates wind turbines from aircraft designs. The majority of today's wind turbines operate within the first 100 m of the earth's surface. This region, which occupies the lowest portion of the planetary boundary layer (PBL), is extremely turbulent and driven by variations, which occur with diurnal changes in atmospheric boundary conditions. The vertical variation of temperature and wind speed with height defines the PBL behavior characteristics.

Tower location and height are the principal factors of system efficiency. Wind average speed depends on many parameters and can vary a lot in the same area. The wind laminar flow over the surface is disturbed by many obstacles and topographic variations. This has two consequences: wind speed decreasing near the earth and turbulences. Both of them diminish as the height increases. A reasonable security margin is 10 m above any obstacle within 100 m. Even in smooth areas, 10 m is advisable [18–26].

2.2. Measurements

The following data were regularly recorded with a time interval daily during the experimental period from the month of September 2002 to August 2003.

- (a) measurement and monitoring on an LCD display of instantaneous power generations of the alternator and all electrical parameters by using electronic energy analyzer,

Table 1

The main characteristics of the elements of the SWTS system studied [7]

No.	Item	Three-bladed rigid hub system
1	Aero dynamic profile form	NACA 63-622
2	Manufacturing material of blade	Epoxy carbon resin
3	Mold use to manufacture blade	Steel
4	Material ratio of blades	50% epoxy resin, 50% carbon fiber
5	Tensile strength (MPa)	900 ^a
6	Average blade weight (g)	1300
7	Number of blades	3
8	Rotor diameter (m)	3
9	Maximum power (W)	1500 ^b
10	Maximum power wind speed (m/s)	12 ^b
11	Cut in velocity value (start up wind speed) (m/s)	2.4 ^b
12	Cut-off velocity (limiting wind speed) (m/s)	18 ^b
13	Theoretical maximum power factor value (dimensionless)	0.4531 ^b
14	Maximum energy conversion (power factor) ratio (dimensionless)	0.35
15	Height of hub (m)	12
17	Roughness of blade surface	Clean
18	Theoretical profile tip lose efficiency (dimensionless)	0.912
19	Theoretical profile lose efficiency (dimensionless)	0.88
22	Power factor range	0–0.35
24	Break system	Mechanical
25	Generator (AC alternator)	1.5 kW Non-synchrony generator/3 phase
26	Power systems	AC/DC/AC and 3 kW inverter
27	Inverter input voltage (V)	96
28	Inverter output voltage (V)	220
29	Inverter output frequency (Hz)	50
30	Generator average Cos Ψ (power factor (P.F.))	0.62
31	Batteries' charging voltage (ΣV)	100
32	Batteries' charging current (ΣA)	22
33	Charge controller disconnect voltage (V)	106
34	Accumulators (batteries)/unit	65 Ah 12 V/ 8
35	Alternative current in the environment lights (ΣA)	0.54
36	Alternative voltage in the environment lights (V)	220
37	Total power of environment lights (W)	100
38	Generator frequency (Hz) (at 4.3 m/s wind speed)	30 ^b
39	Generator average alternative voltage value (ΣV) (at 260 rpm and 10 m/s wind speed)	139
40	Range of rpm of rotor	60–320 ^b
41	Mechanic efficiency of system (dimensionless)	0.97
42	Generator efficiency (dimensionless)	0.98
43	Inverter and power group efficiency (dimensionless)	0.98
44	Gear system efficiency (dimensionless)	—
45	Estimated average decibel value (10 m from hub and average 5.5 m/s wind velocity)	50

^aTheoretical maximum value.^bProduction value.

Table 2
Thermal data used in the example

$C_{p,a}$	Specific heat of air (kJ/kg K)	1.004–1.005
$C_{p,v,1}$	Specific heat of vapor at reference state (kJ/kg K)	1.869
R_a	Gas constant (kJ/kg K)	0.287
R_v	Water vapor constant (kJ/kg K)	0.4615
P_0	Dead state environment pressure (kPa)	101.325
T_0	Dead state temperature (°C, K)	25 °C
$\omega_0, \omega_1, \omega_2$	Humidity ratio of water vapor in air at reference state, state 1 and state 2, shown in Fig. 1 (kg _{water} /kg _{air})	0.098

- (b) measurement of wind velocities at the ground level by anemometer and then these values were calculated for 12 m by using Hellmann equation,
- (c) uncertainty analysis is needed to prove the accuracy of the experiments and an uncertainty analysis was performed using the method described by Holman [27].

The total uncertainties of the measurements are estimated to be $\pm 1.30\%$ for the wind velocities, $\pm 1.02\%$ for voltage and current in the system, and $\pm 3.03\%$ for power factor.

2.3. System operation

Rotor begins to rotate (spine) when the wind speed reaches approximately 2.4 m/s (8.64 km/h). Data sets in which the rotor accelerated from rest up to 250 rpm, which we define as a successful ‘start’, were selected from about 70 h of field test data, yielding 160 starting sequences. Battery charging commences at a slightly higher speed, depending on the battery state of charge. When the battery is fully charged, the charge controller disconnects the turbine from battery. The turbine produces a three-phase alternating current (AC) that varies in voltage and frequency as the wind speed varies. The controller (regulator) rectifies this AC into the direct current (DC) required for battery charging and controls the energy supplied to the batteries to avoid overcharging. SWTS has electronic energy analyzers that show every system status data (phase voltages (V_{LN}), phase currents (I), total current (ΣI), power factor (P.F.) $\cos \Psi$, apparent power, etc.).

3. Analysis

Designing wind turbines to achieve satisfactory levels of performance and durability starts with knowledge of the aerodynamic forces acting at the critical interface between wind and machine.

The efficiency of a wind turbine is usually characterized by its power coefficient as given below, maximum values of C_p can be 0.5926 according to Betz criteria.

$$C_p = \frac{I \cdot V_{LL} \cos \psi}{\eta_{\text{mechanic}} \cdot \eta_{\text{alternator}} \cdot 0.5 \rho \pi R^2 V_r^3} = \frac{P_a}{P}, \quad (1)$$

where C_p is power performance of a wind turbine. The power coefficient is given by Eq. (1). In this study, electrical equipment and mechanic equipment losses were assumed to be $\eta_{\text{alternator}} = 0.98$ and $\eta_{\text{mechanic}} = 0.97$, respectively.

Power performance of a wind turbine can be expressed from fixed angular speed. This parameter is defined by

$$C_M = \frac{C_p}{\lambda}. \quad (2)$$

Wind turbines indicate various C_p values depending on wind velocities. Therefore, their efficiency is best represented by a C_p – λ curve. The tip speed ratio, λ is given by

$$\lambda = \frac{\omega R}{V_r}, \quad (3)$$

where λ is tip speed ratio, R is maximum rotor radius (m), ω is rotor speed (rad/s) and V_r is wind velocity (m/s).

The air flowing with the wind has the same properties as the stagnant atmospheric air except that it possess a velocity and thus some kinetic energy. This air will reach the dead state when it is brought to a complete stop. Therefore, the availability of the blowing air is simply the kinetic energy it possesses:

$$\text{Exergy of kinetic energy} = \text{availability} = \text{ke}_1 = \frac{V_r^2}{2}. \quad (4)$$

To determine the available power, we need to know the amount of air passing through the rotor of the windmill per unit time, the mass flow rate. Assuming standard atmospheric conditions (25 °C, 101 kPa) in this study, the density of air is 1.18 kg/m³, and its mass flow rate is

$$\dot{m} = \rho A V_r = \rho \pi R^2 V_r. \quad (5)$$

Thus,

$$\text{Available power} = W = (\dot{m} \text{ke}_1). \quad (6)$$

This is the maximum power available to the windmill. Most windmills in operation today harness about 20–40% of kinetic energy of the wind [23].

Kinetic exergy is a form of mechanical energy, and thus it can be converted to work entirely. Therefore, the work potential or exergy of kinetic energy of a system is equal to the kinetic energy itself, regardless of temperature and pressure of the environment [23].

Any measured wind velocity value can be estimated for different height by using the following Hellmann equation:

$$V_r = V_{\text{ref}} \left[\frac{H}{H_{\text{ref}}} \right]^\mu, \quad (7)$$

where V_r is the calculated wind velocity, and V_{ref} the wind velocity at reference height. In this study, a Hellmann coefficient (μ) of 0.28 was assumed [24], because tower location is near city.

3.1. Mean time between failures

When a system is often unavailable due to breakdowns and is put back into operation after each breakdown. The mean time between breakdowns is defined as the mean time between failures (MTBFs). During the operating period, when failure rate is fairly

constant, the MTBF is the reciprocal of the constant failure rate [10]:

$$\text{MTBF} = \frac{1}{\lambda}. \quad (8)$$

MTBF is also referred to as the average time of satisfactory operation of the system. In this case, the larger the MTBF, the higher is the reliability of the system. If the reliability factor of the system is to be determined, initially the individual reliability of the subsystems or elements have to be estimated. If each component exhibits a constant failure rate, then the reliability factor for each component will be in the form of exponential $(-\lambda t)$. The t th element will have a reliability of $\exp(-\lambda t)$. Hence, the reliability for the system will be [10,28]

$$R(t) = \exp[-(\lambda_1 + \lambda_2 + \lambda_3 + \dots + \lambda_n)t] = \exp(-\sum \lambda_i t), \quad (9)$$

where λ is the failure rate which is the reciprocal of MTBF, t is time (h). The value of reliability $R(t)$ is 1 at $t = 0$, and it decreases continuously thereafter with time. When ' t ' becomes very large, all the components will fail, thus $R(t)$ will reach a value of zero [10].

3.2. Capacity factor

The capacity factor, which is called the rational efficiency or the overall rational efficiency, is defined as the ratio of the desired actual useful energy production to the theoretical maximum useful energy production:

$$\text{Capacity factor} = \frac{W_{\text{aw}}}{W_{\text{teo}}}. \quad (10)$$

3.3. Performing exergy analysis of the system studied

Exergy is always evaluated with respect to a reference environment (dead state), a restricted form of equilibrium, where only the conditions of mechanical and thermal equilibrium (thermomechanical equilibrium) must be satisfied. This state of the system is called the *restricted dead state*. At the restricted dead state, the fixed quantity of matter under consideration is imagined to be sealed in an envelope impervious to mass flow, at zero velocity and elevation relative to coordinates in the environment, and at the temperature T_0 and pressure P_0 . For computational case, the temperature T_0 and pressure P_0 of the environment are often taken as standard-state values, such as 1 atm and 25 °C. However, these properties may be specified differently depending on the application. T_0 and P_0 might be taken as the average ambient temperature and pressure, respectively, for the location at which the system under consideration operates. Or, if the system uses atmospheric air, T_0 might be specified as the average air temperature. If both air and water from the natural surroundings were used, T_0 would be specified as the lower of the average temperatures for air and water [29]. Exergy efficiency, useful work (P_u), and exergy destruction, can be calculated following Eqs. (11)–(18), respectively. The exergetic efficiency of a turbine is defined as a measure of how well the stream exergy of the fluid is converted into useful turbine work output or inverter work output. We used inverter workoutput as useful work applying this to the wind turbine, we obtain Exergy efficiency:

$$\varepsilon = \frac{W_e}{\text{Ex}_1 - \text{Ex}_2} \quad (11a)$$

or

$$\varepsilon = \frac{W_e}{W_u} \quad (11b)$$

Useful work:

$$W_u = (P_1 - P_2) \frac{\dot{m}}{\rho} \quad (12)$$

Exergy destruction:

$$\dot{E}x_{\text{dest}} = W_u - W_e \quad (13)$$

or

$$Ex_{\text{dest}} = (Ex_1 - Ex_2) - W_e, \quad (14)$$

where the exergy rate

$$Ex = \dot{m}\psi_a. \quad (15)$$

The total flow exergy of air is calculated from Eq. (16) or (17) [30,31]

$$\begin{aligned} \psi_a = & (C_{p,a} + \omega C_{p,v})T_0[(T/T_0) - 1 - \ln(T/T_0)] + (1 + 1.6078\omega)R_a T_0 \ln(P/P_0) \\ & + R_a T_0 \{(1 + 1.6078\omega) \ln[(1 + 1.6078\omega_0)/(1 + 1.6078\omega)] + 1.6078\omega \ln(\omega/\omega_0)\}, \end{aligned} \quad (16)$$

$$\begin{aligned} \psi_a = & [(C_{p,a} + \omega C_{p,v})](T - T_0) - T_0[(C_{p,a} + \omega C_{p,v}) \ln(T/T_0) \\ & - (R_a + \omega R_v) \ln(P/P_0)] + T_0[(R_a + \omega R_v) \ln[(1 + 1.6078\omega_0)/(1 + 1.6078\omega)] \\ & + 1.6078\omega R_a \ln(\omega/\omega_0)], \end{aligned} \quad (17)$$

where the specific humidity ratio

$$\omega = \dot{m}_w / \dot{m} \quad (18)$$

and, T_0 , P_0 are reference temperature and atmospheric pressure which are taken 25 °C, 101.325 kPa in this study, respectively.

4. Results and discussions

Performance data from the wind turbine are stored. Output power and wind speed are sampled over periods of time and average values of wind for each period are stored in wind speed. Table 3 shows measured and calculated performance parameters average values of the SWTS. According to Table 3, actual useful energy measured was 111.8 kWh, and the main reason for this is that moving and light sensors were used on lights for saving energy, and the SWTS was under maintenance some days. Performance test results show that the average wind speed is 7.5 m/s, 616 W and 76 Hz. Electricity is produced by alternator, but power consumptions value is constant always, because total power, voltage, and currents of environment lamps are 100 W, 220 V, and about 0.5 A, respectively [7].

In the present study of wind energy system, there were repetitive machine faults which occurred on the electric, electronic grid feed and mechanic control of the system. A considerable number of the types of faults and problems such as electronic automation, over and lower load electricity problems according to wind speeds and its frequencies,

Table 3
Measured and calculated performance parameters average values of the SWTS [7]

V_r	C_p	\dot{m}	ke_1	$P = (W) = \dot{m} ke_1$	$P_a (W) = C_p * P$	P_e^a	$W_a^{b,c,d}(\text{kWh/month})$
2.4	0.18	20.01	2.88	57.63	10.38	9.16	Sept.–Oct./10 ^c
3.1	0.2	25.86	4.8	124.13	24.8	21.9	Nov./15 ^c
4	0.24	33.36	8	267	64	56.5	Dec./9.8
4.5	0.28	37.53	10.13	380.18	106.45	94	Jan./11.4 ^c
5.5	0.3	45.88	15.13	694.16	208.3	183.9	Feb./10 ^f
7.5	0.35	62.56	28.13	1760	616	544.1	March/20.6
8	0.33	66.73	32	2135	704.55	622.31	April/9 ^g
9	0.3	75.06	40.5	3040	912	805.55	May/8 ^g
10	0.25	83.4	50	4170	1042.5	920.82	June–July/9 ^g
12	0.21	100.09	72	7206	1513	1335	August/9 ^g
						Totals	111.8

^aMeasured value.

^bMeasured value between September 2002–August 2003.

^cMonths.

^dMonthly useful work potential of the SWTS.

^eMoving and light sensors was used on lights for saving energy.

^fSWTS in maintenance.

^gMonthly average wind speed very low for producing electricity at 12 m.

AC/DC/AC invertors losses, mechanic transmission faults in generators, charge controller, mechanic break system faults, roughness of blade surface, batteries' charging voltage problems were experienced, their frequencies briefly are given in Table 3, last column.

The failure rate of the system is found to be $2.28 \times 10^{-4} \text{ h}^{-1}$ and the factor of reliability is found to be 0.37 at 4380 h. The mean time between failures is analyzed and it is found to be 4380 h. It has been estimated that the system reliability factor will become zero at 25,000 h. It was found that by removing 25% of all electric, electronic, and mechanic defects, the failure rate of the system will be reduced to $2.10 \times 10^{-4} \text{ h}^{-1}$ which results in the improvement of lifetime of wind generator from 25,000 to 30,000 h. If 50% of all electric, electronic, and mechanic defects are removed, then the reduction in the failure rate will be $1.5 \times 10^{-4} \text{ h}^{-1}$ and it improves the system life from 25,000 to 35,000 h. It is represented in Fig. 3. If all the defects are further removed by periodical maintenance to an extent of 75%, then the failure rate is found to be $1.3 \times 10^{-4} \text{ h}^{-1}$ which improves the reliability to factor which will become zero only at 40,000 h.

The technical availability is the ratio of operation hours to total machine hours available in a month. The technical availability is almost constant which is around 94.20% in a year. This is because of the electric electronics faults. By minimizing these faults down time and machine down time, the technical availability of the wind turbine generator can still be increased.

The real availability of the horizontal small wind turbine has been analyzed based on total machine hours in the month, excluding machine hours lost due to inadequate wind speed. The real availability is the ratio of generation hours to total machine hours. The real availability is less than 51.67% in a year. This is due to poor wind speed during the period. Since the real availability mainly depends upon the wind speed, the performance gets improved with the higher wind speed. Yearly wind speed frequencies were measured by

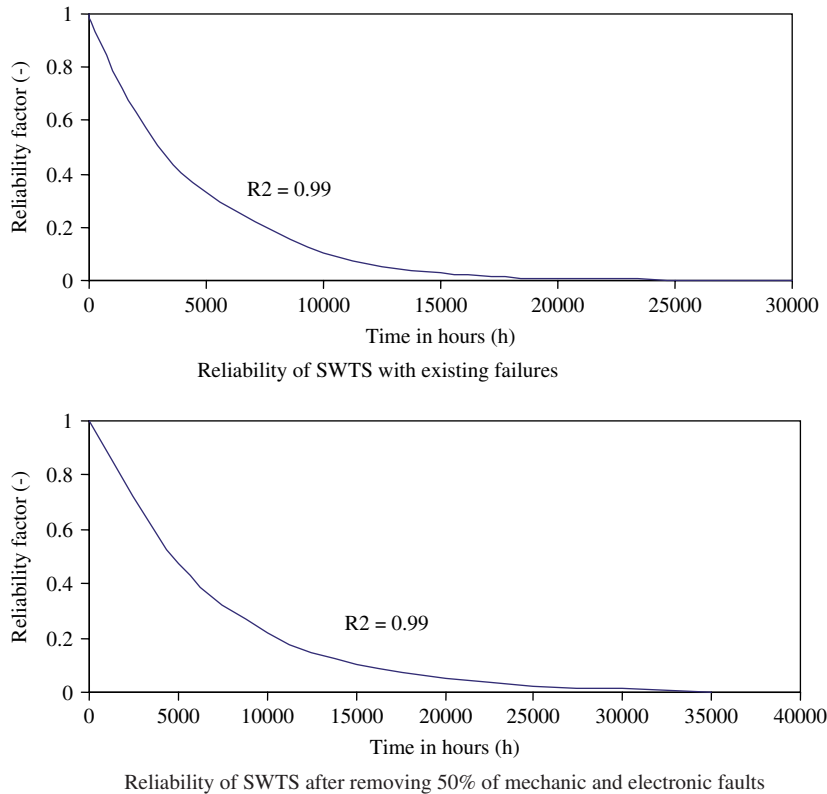


Fig. 3. Reliability of SWTS.

Colak et al. [32]. Their results show that 0–2.5 m/s wind speed duration (Δt_i) is 4234 h and wind speed frequency is 48.33%.

The capacity factor or exergy efficiency has been calculated for the wind turbine generators, using actual generation and installed capacity. The capacity factor is less than 11.58% in a year. During the winter season from the month of November to March, the wind velocity is high and it leads to high capacity factor. This indicates that the capacity factor is also highly dependent on wind velocity. Theoretically useful energy is found as 964.873 kWh (corresponding to measured 1998 wind velocity speeds), and that is the maximum electricity that will be produced in a year; however, actual seasonal performance useful energy was measured as 111.8 kWh from September 2002 to August 2003, and the main reason for the discrepancy is the largely low wind speed frequency distribution, the use of moving and light sensors used on lights for saving energy, and the SWTS was under maintenance some days.

Here, we now analyze exergy efficiencies and their trends. Exergy efficiencies are compared in Figs. 4 and 5. Table 4 and Fig. 4 show that exergy efficiency changes between 0% and 48.7% at different wind speeds by using Eqs. (11a) and (12). Furthermore, 52.3% of the total exergy entering the system is lost, while the remaining 48.7% is utilized at 7.5 m/s wind speed. Nonetheless, maximum energy output (1335 W) and exergy destruction (2876.36 W) are produced at 12 m/s wind speed. Exergy efficiency value of the wind turbine

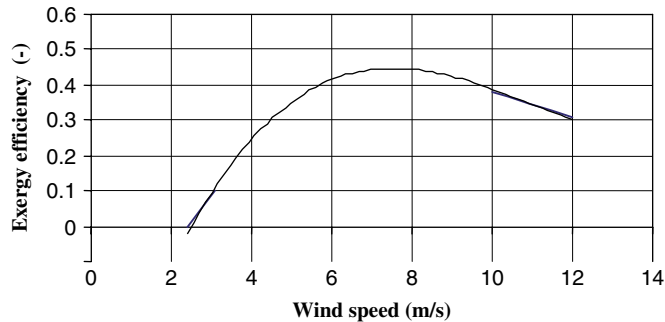


Fig. 4. Exergy efficiency of the three-bladed 3 m diameter horizontal axis wind turbine system, according to wind speed based on pressure differences between state points shown in Fig. 1 (Dead state 25 °C and 101.325 kPa).

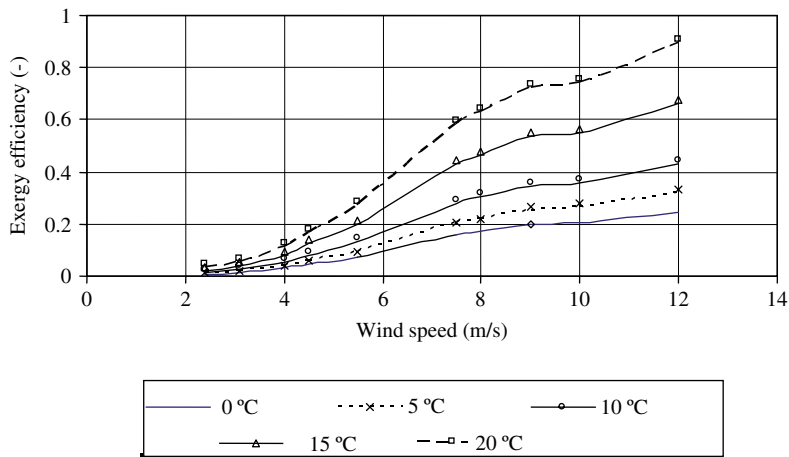


Fig. 5. Exergy efficiency of the wind turbine system, three-bladed 3 m diameter horizontal axis, according to different temperatures of blowing air (Dead state 25 °C and 101.325 kPa).

system, three-bladed 3 m diameter horizontal axis, according to different temperatures (0 °C, 5 °C, 10 °C, 15 °C, and 20 °C) of blowing air can be read from Fig. 5. These values were defined by using Eqs. (14)–(17). According to the graph, exergy efficiency value change between 0% and 89%, and its maximum will be obtained at 12 m/s if wind speed is 20 °C. Fig. 5 presents that blowing air temperature influences the exergy efficiencies, though they are not linear. For the increase of about 20 °C blowing air temperature, the exergy efficiency increases from 24.82% to 89.55%.

5. Conclusions

Although significant progress has been made in developing modern horizontal wind turbines on world, it is necessary to improve research and development facilities in order to develop more efficient, low-cost small horizontal wind turbines which are more reliable and feasible to meet the local energy demands. An experimental system was installed for investigating performance of an SWTS to ensure power supply to some environment lights

Table 4

Exergy, exergy destruction rates, exergy efficiencies and other properties at various wind velocities

Pressure difference at state 1 and 2, ΔP (Pa)	Air flow rate, \dot{m} (kg/s)	Useful power, W_u (W)	Wind velocity, V_r (m/s)	Power at inverter output, W_e (W)	Exergy destruction, Ex_{dest} (W)	Exergy efficiency, ε (–)
2.9	20.01	49.51	2.4	9.16	40.35	0–0.185
10.0	25.86	219	3.1	21.9	197.10	0–0.100
10	33.36	282.50	4	56.5	226.00	0–0.200
9.9	37.53	313.33	4.5	94	219.33	0–0.304
11.2	45.88	435.78	5.5	183.9	251.88	0–0.422
21.1	62.56	1117.25	7.5	544.1	573.15	0–0.487
24.2	66.73	1370.73	8	622.31	748.42	0–0.454
32.1	75.06	2044.54	9	805.55	1238.99	0–0.394
34.0	83.4	2404.23	10	920.82	1483.41	0–0.383
49.6	100.09	4211.36	12	1335	2876.36	0–0.317

Dead state temperature, atmospheric pressure, and density were taken as 25 °C, 101.325 kPa and 1.18 kg/m³, respectively.

of Solar Energy Institute Building. The results obtained during the month of September 2002 till August 2003 were given and discussed. We can extract some concluding remarks from this study as follows:

- In this study, we investigated a small turbine over a period of 15 months, measured a very low capacity factor of 11.58%, and we conclude that wind energy by itself is insufficient to power Solar Energy Institute.
- The exergy and reliability analysis is presented in the paper. The performance of wind turbine generator have been analyzed and the average technical availability, real availability, and capacity factor found from this experimental study are (yearly average) 94.2%, 51.67% and 11.58%, respectively.
- Exergy efficiency changes between 0% and 48.7% at different wind speeds, considering pressure differences between state points.
- Depending on temperature differences between state points exergy efficiencies are found as 0–89%. If failure rate can be decreased, real availability, capacity factor and exergy efficiency will be improved in the system.
- These results show that monovalent central lighting operation cannot be met for all energy needs of Solar Energy Institute Building environment lamps if wind speed is very low. The bivalent or hybrid operation (combined with other lighting systems) can be suggested as best solution in the test location, if peak energy load can be easily controlled.

References

- [1] Tanrioven M. Reliability and cost-benefits of adding alternate power sources to an independent micro-grid community. *J Power Sources* 2005;150(4):136–49.
- [2] Ozgener O, Ulgen K, Hepbasli A. Wind and wave power potential. *Energy Sources* 2004;26:891–901.

- [3] Hepbasli A, Ozgener O. Review on the development of wind energy in Turkey. *Renewable Sustainable Energy Rev* 2004;8(3):257–76.
- [4] Wrixon GT, Rooney ME, Palz W. *Renewable energy*. Berlin, Germany: Springer; 2000.
- [5] Available at: <http://www.nrel.gov/wind/>
- [6] Wright AK, Wood DH. The starting and low speed behavior of a small horizontal axis wind turbine. *J Wind Eng Ind Aerodyn* 2004;92:1265–79.
- [7] Ozgener O. A small wind turbine system (SWTS) application and its performance analysis. *Energy Convers Manage* 2006;47(11/12):1326–37.
- [8] Fuglsang P, Madsen HA. Optimization method for wind turbines. *J Wind Eng Ind Aerodyn* 1999;80:191–206.
- [9] Devinant Ph, Laverne T, Hureau J. Experimental study of wind turbine airfoil aerodynamics in high turbulence. *J Wind Eng Ind Aerodyn* 2002;90:689–702.
- [10] Iniyar S, Suganthi L, Jagadeesan TR. Critical analysis of wind farms for sustainable generation. *Sol Energy* 1998;64:141–9.
- [11] Tangler J, Smith B, Jager D, Olson T. Atmospheric performance of the special-purpose SERI thin-airfoil family. Final results. Solar Energy Research Institute, 1817 Code Blvd., Golden, CO. (Presented at ECWEC 90, Madrid), 1990.
- [12] Cengel YA, Turner RH. *Fundamentals of thermal-fluid sciences*. McGraw Hill; 2001.
- [13] Abbott IH. The drag of two stream line bodies as affected by pro-turbulences and appendages. NACA report 451.1932.
- [14] Abbott IH, Von Doenhoff AE, Stivers LS. Summary of airfoil data. NACA report 824, Langley Field, VA, 1945.
- [15] Jones NP, Raggett JD, Ozkan E. Prediction of cable-supported bridge response to wind: coupled flutter assessment during retrofit. *J Wind Eng Ind Aerodyn* 2003;91:1445–64.
- [16] Hau E. *Windkraftanlagen*. Berlin: Springer; 1996.
- [17] Ozgener O. A review of blade structures of SWTSs in the Aegean region and performance analysis. *Renewable Sustainable Energy Rev* 2005;9(1):85–99.
- [18] Spera DA. *Wind turbine technology fundamental concepts of wind turbine engineering*, vol. 430. 1994; p. 283–98.
- [19] Robinson MC, Tu P. Applied wind energy research at the national wind technology center. *Renewable Energy* 1996;10(2/3):265–72.
- [20] Fujisawa N, Shirai H. Experimental investigation on the unsteady flow field around a savonius rotor at the maximum power performance. Tokyo. *Wind Eng* 1987;11(4):195–206.
- [21] Sadhy D. The application of wind power to irrigation. Brazil. *Wind Eng* 1995; 9(3).
- [22] Sahin AD, Dincer I, Rosen MA. Thermodynamics analysis of wind energy. *International Journal of Energy Research* 2006;30:553–66.
- [23] Cengel YA, Boles MA. *Thermodynamics an engineering approach*. 1994.
- [24] Hapel KH. *Festigkeitsanalyse dynamisch beanspruchter offshore-konstruktionen*. Braunschweig: Vieweg Verlag; 1990 [in German].
- [25] Koseoglu F, Koseoglu T. Ozmak Radio Antenna and Electronic Industry and Trade Co. Sena Electronic Co. Personal Communications, 2003.
- [26] Solener MC, Universal SL. 15kW Velter XV wind turbine user's manual. (Personal fax message to F. Koseoglu), August 27, 2003.
- [27] Holman IP. *Experimental methods for engineers*, 7th ed. New York: McGraw-Hill; 2001. p. 48–143.
- [28] Srinath LS. *Reliability Engineering*. India: Affiliated East-West Press Private Limited; 1991. p. 120–158.
- [29] Moran MJ. *Engineering thermodynamics*. In: Kreith F, editor. *Mechanical engineering handbook*. Boca Raton: CRC Press LLC; 1999.
- [30] Wepfer WJ, Gaggioli RA, Obert EF. Proper evaluation of available energy for HVAC. *ASHRAE Transactions* 1979;85(1):214–30.
- [31] Dincer I, Sahin AZ. A new model for thermodynamic analysis of a drying process. *International Journal of Heat and Mass Transfer* 2004;47(4):645–52.
- [32] Colak M, Gunerhan H, Gunerhan GG. Investigation on the relation between solar energy system and wind and the other meteorological conditions. Ege University Research Found Project No. 93/GEE/007, Izmir, Turkey, 1999 [in Turkish].